Late-Holocene palaeoenvironments of Southern Crimea: Soils, soil-climate relationship and human impact

Fedor N Lisetskii,[1] Vladimir F Stolba[2] and Vitalii I Pichura[3]

Abstract

Occupying 4% of Crimea's territory, the sub-Mediterranean landscapes of Southern Crimea stand out for their distinct soil-climatic conditions and record of human activity. This paper presents the results of study of the newly formed and well-dated soils from 21 archaeological sites, making it possible to build a soil chronosequence covering the last 2.3 ka. To study the natural processes on an intra-secular scale, short series of instrumental meteorological observations were extended, based on dendrochronological records, to a total of 160 years, and the time series of solar activity and energy for pedogenesis were correlated. These data are collated with a 4.2-ka Lake Saki varve record, which was re-analysed applying the DFT spectrum analysis method, with three distinct phases in relative secular variations in precipitation being identified. The phase of a relative climatic stability with moderate variations in precipitation (3.2–1.25 ka BP) was followed by the period of increased moisture (from 1.25 ka BP), unparalleled since the Late Bronze Age. Given the decisive role of increased moisture in the climate-controlled energy expenditures for pedogenesis, in the dynamics of vegetation cover and human ways of life, the identification of these periods contributes to a better understanding of soil–climate relationship and cause-and-effect for nonlinear change in the settlement and landscape history of the region.

Keywords

Black Sea region, Crimea, geoarchaeology, human occupation, lake sediments, Late Holocene, palaeoenvironment, sub-Mediterranean soils

Received 9 November 2016; revised manuscript accepted 7 April 2017

Introduction

The integration of archaeology and the study of ancient soils is pivotal for the reconstruction of palaeoenvironmental conditions and our understanding of human landscape impacts. The study of relict soils that have developed on archaeologically datable surfaces (pedoarchaeology) is particularly helpful in this regard, as well as in establishing the chronology of pedogenesis.

The southern coast of Crimea (SCC) is characterised by climatic and environmental conditions that are very distinct from the rest of the peninsula (Figure 1). The Main Ridge of the Crimean Mountains, which shelters the southern coast, helps create a sub-Mediterranean type of climate, and has also shaped its specific cultural and historical development. Such conditions (relatively stable and generally favourable because of the barrier function of the mountains) make this geographical enclave particularly interesting for studying long-term human–landscape interactions.

Regional soil-genetic investigations provided insights into the evolution of main soil types of the Crimean Peninsula during the Holocene (Kočkin, 1967; Kočkin and Novikova, 1969; Vernander, 1986). However, only recently have pedoarchaeological studies of the sub-Mediterranean soils revealed the particular characteristics of the SCC soils compared with the rest of the Crimean Peninsula (Cordova and Lehman, 2005; Lisetskii and Ergina, 2010; Lisetskii et al., 2013b). In the area of Sevastopol, recurrent patterns of sediment deposition, erosional gaps and soil development over the past 12 ka have been studied in the stratigraphic sections (Cordova and Lehman, 2005).

Palaeogeographic reconstructions of soil evolution have, however, a low resolution which is because of a multistep process:

first, based on multi-proxies, palaeoenvironmental conditions are reconstructed; second, based on the current notion of the relationship between soils and environment, the specifics of pedogenesis in different chronozones are defined; finally, taking into account the obliteration, transformation and inheritance of indicators in the course of pedogenesis, the soil evolution model is proposed.

The growth in regional archaeological and palaeoenvironmental studies in the area (Bilde et al., 2012; Carter, 2002; Carter et al., 2000; Scholl and Zinko, 1999; Stolba et al., 2013; Subetto et al., 2009) has only partially involved the SCC, which remains largely under-investigated. Despite its dead-end position between the sea and the mountains, which limited the mobility of indigenous societies, the southern coast has never been fully isolated, and cultural influence and goods from the steppes and piedmonts drained southwards through the mountain passes. The maritime routes have also been vital in providing access to the SCC. However, the intensity of these cultural contacts, the pressure on the natural landscape and the ecological history of this area were strikingly irregular.

[1]Belgorod State National Research University, Russian Federation
[2]Aarhus University, Denmark
[3]Kherson State Agricultural University, Ukraine

Corresponding author:
Vladimir F Stolba, Aarhus University, Jens Chr. Skous Vej 5, 8000 Aarhus C, Denmark.
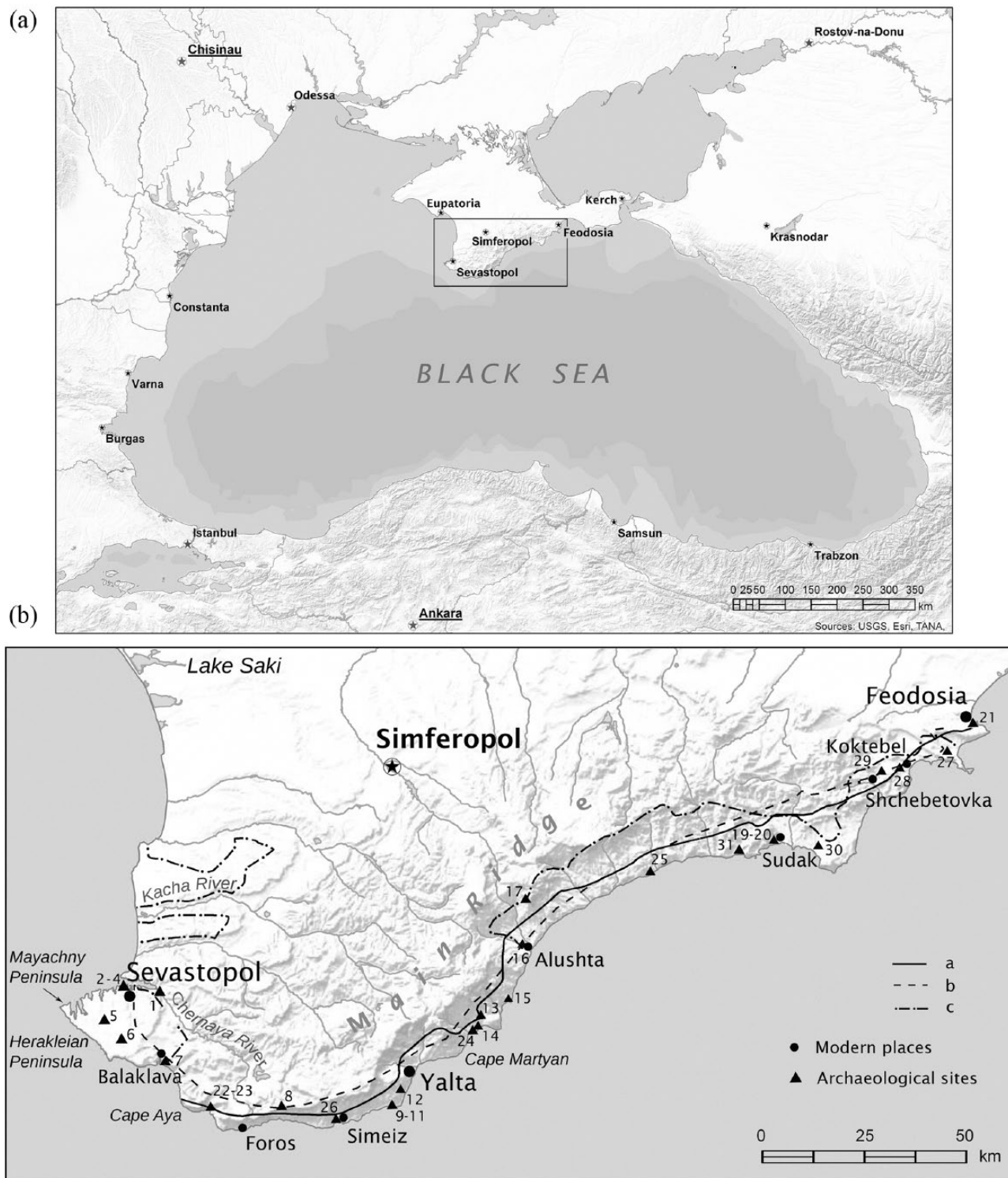Email: klavs@cas.au.dk

Figure 1. The southern coast of Crimea. Limits of the sub-Mediterranean region (a) (after Bagrova et al., 2001: 115), climatic and (b) (after Bagrova et al., 2001: 49) and soil distribution boundaries (c) (after Bagrov and Rudenko, 2004: 30), and archaeological sites: (1–21) sites on which the newly formed (non-buried) soils were studied (see Table 4); (22–31) other sites. Key: (1) Kalamita, (2–4) Chersonesos, (5) Chersonesean farmhouse on plot 197, (6) Chersonesean farmhouse, Berman Ravine, (7) Chembalo, (8) Isar-Kaya, (9–10) Charax, (11) Ai-Todor, (12) Oreanda-Isar, (13) Kizil-Tash, (14) Artek, (15) Cape Plaka, (16) Aluston, (17) Funa, (19–20) Sudak, (21) Feodosia, (22–23) Laspi 1 and 7, (24) Gurzufskaya Krepost, (25) Ardych-Burun, (26) Mt Koshka, (27) Ordzhonikidze, (28) Koktebel, (29) Chelki, (30) Kapsel and (31) Kutlak.

Taking a geoarchaeological approach, this article examines the Crimean sub-Mediterranean soils, soil-climate relationships and human impact on the natural landscape. The pedological studies were conducted at 21 archaeological sites of the SCC and concerned the soils which formed on their surface over the past 2.3 ka (Figure 1). To better understand the complex soil-climate relationships, the main trends in the long-term climate variability in the region will be re-examined, based on the climatic record from the instrumental period and proxies such as tree rings and the sedimentation rate data from Lake Saki (western Crimea; 45.118646N, 33.548381E).

Study area

Geographical setting

The SCC is about 180 km long, extending from Cape Fiolent in the west to Cape Ilya in the east (Figure 1). Sheltered by the Main

Table 1. Climatic characteristics of Crimea and the Mediterranean (modified from Bagrova et al., 2001).

Weather station	Air temperature, °C		Relative humidity in July, %	Average number of summer days with precipitation
	January	July		
Sevastopol	2.5	22.4	69	8.0
Yalta	4.0	23.7	61	5.2
Feodosia	1.8	24.2	64	12.0
Antalya	9.9	28.1	62	0.0
Limassol	11.7	25.6	60	0.0
Athens	8.3	26.7	48	3.0
Marseille	6.1	22.2	54	3.0

Table 2. Climatic characteristics of the southern coast of Crimea (modified from Berezina, 1967).

Meteorological observation points	T1	T2	T3	T4	Annual evaporability (I), mm	Sum of precipitation in June – September, mm	Annual precipitation (P), mm	K = P/I	Q
Sevastopol	22.4	2.6	38	12.0	835	104	349	0.42	953
Foros	23.6	4.1	37	13.3	1115	109	422	0.38	1072
Yalta	23.7	3.8	39	13.0	1025	133	635	0.62	1380
Alushta	23.3	2.9	39	12.3	930	114	427	0.46	1121
Sudak	23.2	1.8	38	11.9	965	106	318	0.33	864
Feodosia	23.8	0.5	38	11.7	935	138	376	0.40	1054

T: temperatures, °C; T1: average of the warmest month; T2: average of the coldest month; T3: absolute maximum; T4: average annual; Q: climate-controlled energy for pedogenesis, MJ m^{-2} yr^{-1}.

Ridge of the Crimean Mountains, it occupies the coastal band to an altitude of 400 m a.s.l. The landscape is dominated by sub-Mediterranean forest-shiblyak vegetation, which occupies 1255 km² along a 1–15 km-wide band in the lowest parts of the slope. The steepness of the southern slope results in high rates of erosion, which are accelerated by human impacts, notably overgrazing. Of the calcaric Cambisols in this area, 69% are eroded (Kočkin and Novikova, 1969).

Climatic conditions approaching the 'Mediterranean climate type' are only observed in Crimea on a 50-km-long stretch west of Yalta and to an altitude of 70–80 m a.s.l.: the average temperature in January is above 4°C, the sum of active temperatures is over 3600°C and the sum of precipitation in the cold period (October–May) exceeds that of the warm period (June–September) (Bagrova et al., 2003) (Table 1). The peripheral areas of the SCC are colder, particularly in the east, where conditions are drier and where cold period precipitation amounts to 63–67%. In contrast, in the centre of the SCC, precipitation in the cold period is 73–79% (Table 2). While the hydrothermal coefficient for the entire SCC is 0.6 on average, the precipitation-evaporation ratio in its peripheral parts does not exceed 0.46, and only in the central areas (Yalta) does it reach 0.62 (Table 2).

Despite its relatively small area, Crimea possesses a diverse mosaic of ecological conditions, which supports a wide diversity of flora. Along with 127 endemic species and subspecies (Ena et al., 2007), the Crimean flora comprises many Mediterranean species (evergreen trees and scrub such as *Arbutus andrachne* L., *Juniperus excelsa* Bieb., *Taxus baccata* L., *Ruscus hypoglossum* L. and *Cistus tauricus* J.Presl & C.Presl). In the shrublands and woodlands along the south coast, arborescent juniper grows side by side with pubescent oak and strawberry tree (*Arbutus andrachne* L.). The forest occupying the lower terraces here consists of *Juniperus excelsa, Arbutus andrachne, Quercus pubescens* and *Pistacia mutica*. The appearance of pistachio is linked to warm climate conditions and its occurrence has expanded in the last 7 ka (Cordova and Lehman, 2005).

In terms of the soil types, the SCC constitutes the Crimean subtropical forest soil zone. Calcaric Cambisols (IUSS Working Group WRB, 2014), or, according to the nomenclature of Crimean soils, the cinnamonic forest soils, occur on the southern slope of the Main Ridge and in the foothills west and east of it. The total area in Crimea occupied by calcaric Cambisols is 48,500 ha (Kočkin and Novikova, 1969). The parent materials are clayey schist, limestone and conglomerates. Throughout the territory of Crimea, three subtypes of Cambisols can be distinguished: the typical, the leached (non-calcareous) and the calcareous, with the third of these making up 67% of the total area of Cambisols (Bagrova et al., 2003). Alternatively, Kočkin (1967) distinguishes between 11 widespread varieties of Cambisols in the mountainous Crimea. The most widespread of these are calcaric Cambisols on weathering crust and hillwash of parent rocks (66.6%), followed by similar but non-calcareous soils (29.3%), and finally by the salty mountain soils on hillwash of parent rocks (4.1%). Only about 15.5% of Cambisols are on land in cultivation.

On the Herakleian Peninsula (Figure 1), calcaric Cambisols are marked by a lighter A horizon, carbonates at 20–50 cm depth, a diffuse transition to the underlying horizons (B1t, B2, BC$_{Ca}$; 50–150 cm), gleysation and biochemical recovery of Fe, Mn and so on. The *terra rossa* soils, also termed sodic calcareous soils (Vernander, 1986) or reddish cinnamonic clay-and-gravel soils (Kočkin, 1967), are formed on detrital limestone and chalks under grassy vegetation. Reddish Cambisols on the Mayachny Peninsula and on the southern slope of the Main Ridge are considered modern rather than relics of the Palaeogene and Neogene (Kočkin, 1967).

Archaeological setting and human impact on the landscape

While the earliest evidence of human habitation in the area dates back to the Mesolithic (Telegin, 1985), it is not until ca. 7–5 ka BP that intense human disturbance becomes traceable, indicated, for example, by the establishment of the phrygana vegetation (the Mediterranean type vegetation dominated by xerophilous low shrubs) (Cordova and Lehman, 2006). Significant changes in human ways of life around that time are also suggested by

archaeological record. Fossil wheat grains found at Ardych-Burun and AMS ^{14}C dated to 3652–3349 cal. BC represent the earliest reported evidence of cereal consumption in Crimea (Motuzaite-Matuzeviciute et al., 2013). Along with a primitive bone hoe found at Laspi 7 (Telegin, 1985), this might be seen as evidence of an expansion of the local Chalcolithic population's economy beyond the conventionally assumed pastoralism, hunting and exploitation of marine resources.

In the Bronze Age (ca. 4.9–2.9 ka ago), signs of human habitation in the area remain insignificant. Except for Mt Koshka near Simeiz and some findspots in the area of Sevastopol (Stupko, 2011), the sites are located at the eastern periphery of the SCC: Ordzhonikidze, Koktebel, Chelki, Kapsel and so on. (Kolotuchin, 1996, 2003; Schultz, 1957) (Figure 1). Pastoral transhumance, common to all Mediterranean countries, is likely to have been a normal livestock practice here too. According to the archaeozoological data from the Crimean steppes and piedmonts, cattle prevailed in the Bronze Age pastoralists' herd, constituting 44% of the herd in some places (Bibikova, 1970; Kolotuchin, 1996, 2003). This might account for the observed pattern of the Bronze Age habitation along the coast, as the more gentle terrain of the SCC's western and eastern peripheries with easier access to the Yaila and steppe pastures is better suited to such types of livestock. Although the lack of data does not permit any rigorous assessment of agricultural activity in this period, major slope destabilisation and soil erosion, a decrease in arboreal vegetation as well as a notable increase in phrygana observable in the later Bronze Age (3.5–3 ka BP) (Cordova and Lehman, 2005) suggest accelerated runoff and human impact.

The Greek colonisation of Crimea had little impact on most parts of the SCC. This is probably because this land was occupied by the Taurians, who gained fame in the ancient narrative through their savagery and atrocity towards foreigners (Herodotus 4.99, 103). Although post-antique abandoned lands preserve the footprints of agrogenesis even after two millennia of recovery (Lisetskii et al., 2015), the impact of the Taurians on the environment of the SCC is still difficult to estimate. It was probably not significant though, given that the overwhelming majority of the Taurian (Kizil-Koba Culture) sites are situated in the foothills north of the Main Ridge (Kolotuchin, 1996; Kris, 1981). An exception to this pattern are the surroundings of Balaklava and the Herakleian Peninsula, where indigenous sites are known along the periphery of the Greek rural territory until ca. 2.35–2.3 ka ago (4th century BC), after which point they vanish, and the population migrates to the north-western Crimea (Kravčenko, 2008; Ščeglov, 1981; Stolba, 2002). Written sources suggest, however, that some Taurians inhabited the area of Balaklava until Roman times (Stolba, 1993, 2014), although archaeologically they remain mute.

Almost a century and a half of Roman presence in the region (1st–3rd centuries AD) left no marked imprint on its soils that persists to the present. Their watch and signalling posts on the periphery of the Herakleian Peninsula as well as garrisons in Chersonesos, Balaklava and on Cape Ai-Todor (Charax) protected the borders of the allied Chersonesos and strategic communications (Zubar, 2001–2002). Material retrieved in the excavations of Charax (Blavatskij, 1951; Novičenkov and Novičenkova, 2002) suggests that fishing and perhaps some subsistence farming near the fortress walls were among a few economic activities of its garrison. Given its position on a rocky promontory as well as the military and navigational functions of this coastal fort, a broader agricultural expansion of its occupants into the surrounding territory seems very unlikely.

The period of the most active use of the Alushta Valley falls in the 2nd through the 3rd centuries AD, as suggested by a significant number of indigenous sites discovered by archaeological surveys (Lysenko, 2010). Spread throughout the valley at a distance of 2.4–8.5 km from the sea and an altitude of 70–620 m a.s.l., they occupy places near water sources most convenient for life and less vulnerable to the risk of coastal natural hazards. The absence of synchronous cemeteries suggests economic activities which required periodic changes of place (Lysenko, 2010). The third-century invasion of the Alans and Goths put an end to the bulk of the Alushta Valley sites and to over a century-long Roman presence in Crimea (Myc, 1989). After the withdrawal of the Goths, the Byzantines left their mark on the coast in the 6th century, and in the 14th century, the Genoese began to establish their colonies at different points on the SCC (Myc, 1991).

The most distinct anthropogenic transformation of the landscape and soils occurred on the Herakleian Peninsula, which from the 4th century BC (ca. 2.4–2.3 ka BP) through the Roman period constituted the nearer *chora* (rural territory) of Chersonesos and was divided into a system of rectangular plots (Carter et al., 2000; Lisetskii et al., 2013b; Nikolaenko, 2006). Unlike the city's distant *chora* in the north-western Crimea, which was its main granary, this area's main specialisation was viticulture and production of wine. The palaeobotanical finds suggest the domestication of wild local species of grapevine that were hardier and better adapted to the conditions of Crimea than Mediterranean species (Januševič, 1986; Yanuchevitch et al., 1985). Olive pollen is missing in the palynological records of southwestern Crimea (Cordova and Lehman, 2003). In the local context, the place of olives, which along with cereals and grapes constituted the Mediterranean triad, was occupied by pulses (Januševič, 1986; Stolba, 2012). Yet here too, periods of intensification alternated with periods of decline and desolation caused not only by military raids and socio-political insecurity but also by climate change (Stolba, 2005a, 2005b, 2012). This proves that the model of nonlinear change suggested for the settlement and landscape history of Greece (Butzer, 2005) is fully applicable to the SCC too.

Material and methods

Soil chronosequences were established in the course of studies at 21 archaeological sites situated within the SCC and dated from the 3rd century BC to the early 20th century AD (Figure 1). Soils were studied in sections that revealed the entire soil profile formed after the end of archaeological occupation or the last addition for earthen structures (Figure 2).

The age of each site was determined archaeologically (coins, amphora stamps or other narrowly datable pottery; sites 4–6, 8–19) or based on historical record (sites 1–3, 7, 20–21). The accuracy of archaeological datings which serve as *terminus post quem* for the chronology of the newly formed soils is nowhere more than 25 years, and in some cases, it is less. Because of the natural variability of the humus-horizon thickness, the accuracy of the soil-genetic dating employed in our study is ±100 years. This dating technique is based on the concept of a soil chronofunction (Jenny, 1980) which describes the mathematical relationship between time and certain irreversible genetic soil properties (e.g. thickness of soil horizons, biogeochemical indicators, etc.) (Lisetskii et al., 2016). These relationships are unique for each region with specific conditions of pedogenesis. A soil chronofunction for the SCC has been established in Lisetskii et al. (2013b). Chemical analyses of soils formed on the surface of each of the 21 sites included the following standard procedures: the organic matter (OM) after Tyurin, the bulk nitrogen content (N) after Kjeldahl, CO_2 in carbonates by acidometry and labile compounds of phosphorus after Machigin (Arinushkina, 1970). Bulk chemical composition of the soils and rocks was measured by XRF (Spectroscan Max-GV) in powdered specimens.

Figure 2. The Roman fortress of Charax (AD 1st–mid-3rd centuries): (a) fragment of the lower defensive wall (left) and (b) soil section (no. 10) atop the defensive wall (right).
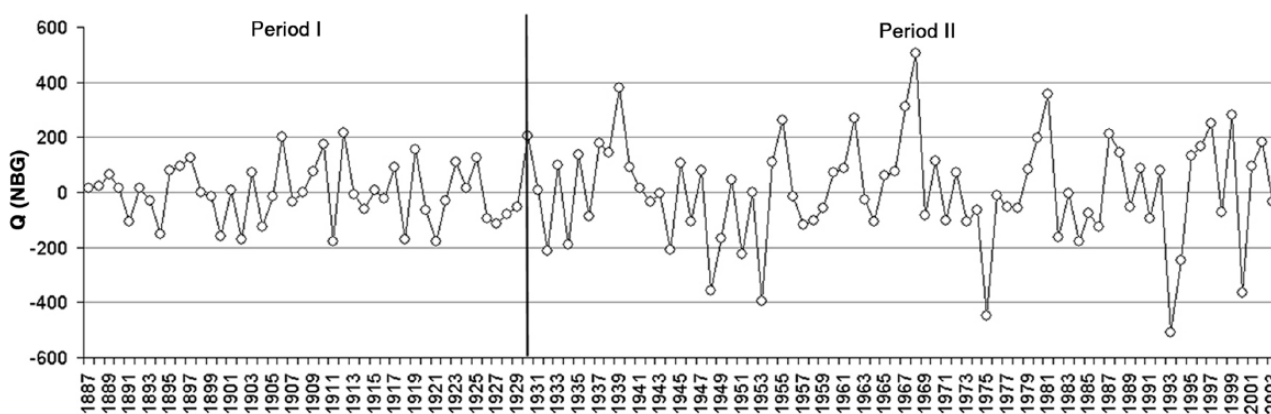

Figure 3. Dynamics of long-term changes of energy expenditure for pedogenesis observed at the Nikitsky Botanical Garden (Q[NBG], MJ m^{-2} a^{-1}) without the trend component. Periods I and II – sub-centennial periods.

According to Volobuev (1975), the climate-controlled energy for pedogenesis (Q) is determined by the annual radiation balance of the active surface (B) and the sum of precipitation. After correction of his equation (by introducing factors to express B in the international system of units), the climate-controlled energy for pedogenesis can be calculated by the equation:

$$Q = B \cdot \exp\left(-1.23\frac{B^{0.73}}{P}\right) \qquad (1)$$

where B = radiation balance (MJ m^{-2} yr^{-1}); P = annual sum of precipitation (mm).

This approach reflects the relationship between the parameters of soil profiles and hydrothermal factors and their limiting combinations more accurately than a multiplicative approach where the parameters of heat and moisture are multiplied without weight coefficients (Rasmussen et al., 2005). The estimates of Q made using Volobuev's equation were compared with those based on the Effective Energy and Mass Transfer (EEMT) method by Rasmussen (Rasmussen and Tabor, 2007).

To reconstruct the climate of the last 2500 years on the basis of a 117-year long climate alteration record, wavelet transform for decomposition of the initial series into high-frequency (HF, approximating) and low-frequency (LF, refining) signals and Fourier transform were used. Based on this procedure, the basic harmonic components were defined, and by determining sinusoidal components at different frequencies, the variation in Q was reconstructed. To identify the genetically significant harmonic oscillations at different levels of localisation, the decomposition of empirical series to the level of discernible LF, HF and trend components, as well as discrete wavelet transform (DWT) and multiple-scale analysis, was performed. The evaluation of the initial signal preservation, using the global threshold compression method, demonstrated symlet wavelet transform to be the most effective function here, preserving 98.9% of the LF signal. Smoothing of non-significant local outliers, in order to define the basic intra-secular harmonics of changes in Q, was conducted using the Parzen-window method.

The aforementioned 117-year long climate alteration series is a composite record. Since the main SCC's weather station at the Nikitsky Botanical Garden (NBG) presents a shorter series of observations than that in Simferopol, we extended the series of Q values by extrapolating the Simferopol data on the SCC. The collation of the data pertinent to the energy expenditures for soil formation, which was retrieved at both weather stations in the period 1932–2003, has demonstrated a generally close interrelation (r = 0.70) between the two variables (Figure 3), the average values for the SCC being 175 MJ m^{-2} higher. Hence, the dynamics of climatic processes and of those dependent on them can be considered together for both the northern and the southern foothills of the Crimea.

The analysis and simulation of the climate-indicator dynamics were carried out using modules *Basic Statistics, Time series and forecasting* (TSF) and *Neural Networks* of the STATISTICA 10.0 software. Generalised regression neural network (GRNN) analysis

(Haykin, 2008) was used for nonlinear estimation. The synchronism between the rhythms of solar activity and the climate-controlled energy for pedogenesis was evaluated using a trend approach for smoothing time series. The smoothing was performed in the statistically normalised sequences using the formula:

$$\text{Norm}(X) = \int_{1}^{t} \frac{(x_i - \bar{x})}{\sigma} + 3di \qquad (2)$$

where $\bar{x}$ = multi-annual mean value; σ = standard deviation (SD).

Tree-ring widths have considerable potential for reconstructing past climate and precipitation regimes at a specific site (Fritts, 1976; Michaelsen et al., 1987; Zhang, 2015). The examination of tree-ring widths (R) of *Juniperus excelsa* from Yalta for the years 1844–1994 (Lovelius and Grican, 1998) and the correlation found between the Q and R values over the period of 1887–2003 allowed us to reconstruct the Q values over the additional 44 years (1844–1887).

To comprehend the conditions of pedogenesis on the SCC and to help interpret climatic and hydrological events, the reconstructed 161-year long climatic series was compared with pollen diagrams from Lake Saki (Gerasimenko and Subetto, 2007). The fact that western Crimea falls within the same local zone of European seasonal temperature anomalies as the Lower Dnieper region (Luterbacher et al., 2004) also made it possible to collate Lake Saki sedimentation rates with the water discharge of the Dnieper River to establish the main trends of environmental change on the SCC during the late Holocene (Fedorov, 2010; Lisetskii et al., 2013a; Švec, 1974). We use these as a basis for comparing with our pedoarchaeological data. Having converted Šostakovič's (1934) original data on the varve thickness in the Lake Saki bottom deposits to the rainfall scale suggested by Brooks (1949), Lamb (1977) has produced rainfall variations in Crimea over the past 4.2 ka. These data have been subjected to a detailed statistical analysis both in a 10-year sampling interval (Xanthakis et al., 1995) and on an annual basis (Liritzis and Fairbridge, 2003).

To present climatic signals of the last 2500 years from the lake sediment data provided by Šostakovič (1934) and the AMS 14C dated cores retrieved in 2005, wavelet transform for decomposition of the initial series into HF (approximating) and LF (refining) signals as well as Fourier transform were used. This made it possible to focus on local characteristics of the processes analysed, which cannot be identified by traditional transforms presented, for example, in Xanthakis et al. (1995).

For each basic wavelet, the integral wavelet transforms of the time series *f(t)* defined within the interval of $-\infty \leqslant t \leqslant +\infty$ are expressed as:

$$(W_\varphi f)(b,a) = |a|^{-\frac{1}{2}} \int_{-\infty}^{\infty} f(t) \overline{\varphi\left(\frac{t-b}{a}\right)} dt \text{ with } a,b \in R, a \neq 0 \quad (3)$$

where $\varphi(t)$ is function of wavelet transform, a is time scale and b is time shift.

Using continuous transform, signal $\varphi(t)$ is transferred from a two-dimensional into a three-dimensional space with the coordinates time (b), scale (a) and amplitude (c). In this procedure, the signal is decomposed into harmonics with frequencies corresponding to the scales (a).

Results and discussion

Development of soils over time

The response of soil properties to the climate variations can be rapid or slow, and some responses are persistent while others are transient. The hydrothermal regime, the type of humus, the carbonate and salt profile as well as the organic and mineralogical composition require their own interval of time for a certain process to reach a relative equilibrium with environmental factors. Therefore, the chronological organisation of the soil system is realised via a number of hierarchical levels of characteristic times (CTs): $n \cdot 10$ years; $n \cdot 100$ years or $n \cdot 1000$ years (Goleusov and Lisetskii, 2009).

The CTs of different soil indicators (composition, properties and processes) differ. For the composition of the soil solution, CT is measured in hours; for the contents of OM, it is measured in hundreds and thousands of years, while the CT of the decomposition of the primary minerals is measured in thousands of years. The CTs of the same indicator vary considerably in different bioclimatic conditions. Thus, one can speak of progressive evolution, when the bioclimatic potential of the subsequent stage exceeds that of the previous stage.

Since most of the soils in the world had a long formation period, the direct observation and study of pedogenesis at the level of micro-processes (physical, chemical and biological) are impossible. Hence, the processes that form soil indicators need to be studied according to the following scheme: factors → processes → properties. Climatic factors determine the development of the soil profile corresponding to their impact energy characteristic of the given geo- and topographic situation, climate and parent material. On carbonate rocks, the thickness of the soil's genetic horizons depends on time, gradually growing with age, that is, a progressive evolution of the soil profile takes place.

While eutric, lithic and rendzic Leptosols predominate on limestone in the Mediterranean, the narrow band of mollic Leptosols encircles the limits of the SCC. These mollic Leptosols form under dominant herbaceous cover. This accounts for the humus content in the upper soil horizon, which amounts to 4% on average (ranging from 2.0% to 7.8%); bulk phosphorus in the layers of 0–10 cm and 20–30 cm reaches 0.23% and 0.14%, respectively, the amount of labile phosphorus throughout the profile being 0.3–4.5 mg per 100 g. The upper horizon contains 2.7% of bulk potassium, while the quantity of labile potassium varies considerably from 12 to 108 mg per 100 g (Kočkin et al., 1972).

None of the usually expected transformations of soils formed under forest vegetation (increased acidity of the water solution, smaller contents of humus and fulvates) are observed when comparing closely positioned Cambisols under the mesophytic herbs and grass vegetation (near Balaklava) and under the pine-juniper forest ('Cape Aya' park) (Table 3). Among Cambisols, the brightest red hue (5YR 5/6 (6/8) on the Munsell scale) develops in those formed on a red, *terra rossa*-type weathering crust and hillwash of limestone rocks (Cape Martyan and some other localities on the SCC; Figure 1). Although weathering also occurs in the upper soil horizon, it is less intense here because of this layer's dryness. Colloidal substances are actively formed in the underlying reddish-brown metamorphic horizon Bw (27–40 cm) and account for its specific physical properties.

The distribution area of Cambisols in Crimea expands to the *cuesta* and *shiblyak* landscapes of the piedmont forest-steppe, including the Herakleian Peninsula (Figure 1). In some parts of Crimea, where the Holocene soils were identified as Cambisols, they are not Cambisols as far as their properties are concerned (Cordova and Lehman, 2005).

Among the main Crimean soil types, calcaric Cambisols stand out for their low late-Holocene formation rates, closing in that respect the following descending sequence: (1) calcic Chernozems and calcic Kastanozems, (2) eutric Cambisols and (3) calcaric Cambisols (Lisetskii and Ergina, 2010). The data from 21 soil sections on the SCC give, according to the data approximation model (Lisetskii et al., 2013b), an estimated average increase of the humus-horizon thickness during the first 2300 years of the soil formation of 0.047 mm a^{-1} or about 0.6 t ha^{-1} a^{-1}.

Table 3. Chemical properties of Horizon A of Cambisols under steppe and forest.

Soil indicators	Steppe	Forest
Munsell colour (dry)	7.5 YR 5/6	10 YR 6/2
$CaCO_3$, %	10.87	6.86
OM, %	3.58	5.73
N total, %	0.416	0.406
C/N	9	14
pH (H_2O)	7.8	7.5
P_2O_5, mg kg^{-1}	27.7	22.0
Adsorbed bases (mmol dm^{-3} per 100 g)	28.3	30.7
Ratio of Ca in the soil absorbing complex, %	94	87
C_{ha}, % of C	8.2	12.7
C_{fa}, % of C	19.5	17.4
Contents of macro- and microelements (%):		
CaO	5.77	5.15
P_2O_5	0.46	0.17
K_2O	1.86	2.50
Fe_2O_3	6.33	5.37
Al_2O_3	11.61	14.68
MnO	0.20	0.07

OM: organic matter; C_{ha} and C_{fa}: carbon contents of humic and fulvic acids, respectively.

Because of the Mediterranean-type climate, the Holocene non-eroded soils of the SCC are distinguished by intensive fixation of humus in the upper horizon, where it amounts to up to 10%, occasionally up to 13%. Notably, the considerable accumulation of humus is observed already in the few-centuries-old soils (Table 4). In the chronological series of soils aged from 500 to 11,500 years, the amount of humus in the upper horizon increases from 4.1% to 7.0–9.6%. The average rate of humus accumulation in the upper horizon of Crimean Cambisols can be estimated as 0.037%/100 a (Lisetskii et al., 2013b).

In extraglacial zones, current soil processes superimpose onto the previously formed soils which, in this case, serve as a parent material, being isolated from the new pedogenetic factors. Calcaric Cambisols can be defined as lithogenic soils characterised by a high significance of ancient substrates. Their texture varies from silt loam to clay loam and clay (Kočkin et al., 1972). They typically contain skeletal particles such as rubble and stones in quantities that decrease up-profile. Soil solutions obtained from the top horizon are mostly neutral (pH = 6.8–7.0), becoming alkaline lower down (pH = 7.5–7.7). The complex absorption is mostly because of calcium (80–90% of the total of the bases).

The character of the aqueous, salt, oxidation-reduction and other regimes serves to diagnose the current soil processes. An elementary soil process is, however, more complex than a micro-process, being a combination of micro-process and concealing both past and present effects.

One of the characteristic features of Cambisols of the SCC is their relatively narrow molecular ratio SiO_2:R_2O_3 (4–5), which further declines in the lower sections of the profile. Because of considerable differences in the content of SiO_2, different ages of the soils at archaeological sites are easily identifiable through the accumulation of Fe oxides and especially of Al oxides (Table 5). Because of periodical washing, the leaching of easily soluble salts and carbonates takes place. Correspondingly, the values of the eluviation coefficient (C_e) of the soils, whose determination was proposed based on the equation C_e = SiO_2:(RO + R_2O) (Liu et al., 2009), increase towards the soil age of 1.9–2.2 ka ago (Table 5).

Climatic changes and the energetics of pedogenesis

The weather data series from the instrumental period provides a picture of modern climate change. The data from the area of the NBG (Korsakova, 2011) demonstrate that the sums of active air temperatures higher than 10°C ($\Sigma t > 10°$) had two maxima in the period of 1930–2007: in 1966–1968 and in 2001–2007, when the augmentation of $\Sigma t > 10°$ amounted to 215°C as compared with an average of $\Sigma t > 10°$ in the 78-year period (ca. 3645°C). Since 2001, the recurrence and duration of high air temperatures (above 25°C and 30°C) have markedly increased. The modern-day (1930–2007) changes in climate on the SCC can be characterised as a warming accompanied by some increase in precipitation. The simultaneous increase in heat provision and rainfall constitutes the major trend in the modern climate change. As shown by Cordova and Lehman (2005), the climatic conditions conducive to the formation of Cambisols existed in the Neolithic, Chalcolithic and Bronze Age, while at the turn of the Bronze Age and Iron Age, Rendzinas began to develop. In the period following the last significant aridification (2.4–1.8 ka BP), pedogenesis on the SCC proceeded in conditions corresponding to the sub-Mediterranean ones.

The reconstruction of the rhythms of pedogenesis and the changes in the climate-controlled energy expenditures for soil formation (Q) is presented in Table 6. Combining the maximum thickness of the humus horizon (H_{lim}) with climate-controlled energy expenditures for soil formation and the character of parent material will make it possible to predict the trends of pedogenesis and humus-horizon formation rates at secular and multi-secular levels.

Based on the data from the instrumental period, an exponential relationship between Q, as calculated according to the methods of Rasmussen and Tabor (2007) (Q_R) and Volobuev (1975) (Q_V) has been established: $Q_R = 52.065 \exp(0.001 \cdot Q_V)$, $r^2 = 0.93$. Hence, these approaches prove to be mutually complementary. However, Volobuev's method ensures an additional possibility to define the effect of climate on the formation of soil profile.

Taking into account the dependence of the maximum humus-horizon thickness (H_{lim}) on energy expenditures for soil formation (Q) and contents of particles measuring <0.01 mm (PC, %), the contribution of climate changes to the formation of soil profile can be estimated:

$$H_{lim} = \frac{3914.6 \cdot PC^{-0.19}}{1 + e^{(5.35 - 0.00523 \cdot Q)}} \qquad (4)$$

Considering PC a constant of 75% for the dominating clayey parent material (Lisetskii et al., 2015), potential variations in the humus-horizon thickness (ΔH_{lim}) have been estimated (Table 6).

Using current parameters of the regional climate as a reference point, the negative secular tendency in the change of the climate energy potential (Q) prevailed over the positive one (1350 years or 54% vs 1150 years or 46%) during the last 2500 years. This might have determined the respective variations in the soil profile development (ΔH_{lim}, mm). The soil memory may have retained the signals of processes with CT of centennial order such as humus accumulation, eluviation, decalcination, soil structure formation and so on.

The instrumental climate observations in the western Mediterranean demonstrate that a better moisture provision is often inversely related to temperature (Maheras, 1988, 1989). Therefore, a synthetic indicator is required to reflect the nonlinear influence of the conditions of heat and precipitation upon biological and biomineral systems, including soils. An analytical equation by Volobuev (1975) (equation (1)), which still retains its validity (Alyabina and Nedanchuk, 2014; Rasmussen, 2012), permits the use of the values of annual sums of precipitation and radiation balance for the estimation of climatic expenditures expressed in energy units Q (MJ m^{-2} a^{-1}).

The intra-secular periodicity of pedogenesis and changes in soil properties are measurable in decades and correlate with the

Table 4. Parameters of soil chronosequences at archaeological sites of the SCC with sub-Mediterranean conditions.

Archaeological site[a]	Object	Vegetation[b]	Parent material[c]	Soil age, years	Horizon, levels, cm	C_{org}, %	A + AB, mm	ΔH, mm yr^{-1}
3. Chersonesos	Battery	MHG	L	105	AU, 0–7	7.42	70	0.667
2. Chersonesos	Battery	M	L	158	AU, 0–11	6.79	107	0.677
20. Fortress Sudak	ruins of barracks	MHG	WC	200	–	–	100	0.500
1. Kalamita	Glacis	M	L	362	AU, 0–14	6.44	140	0.387
8. Isar-Kaya	Fortress	F	WC	500		–	160	0.320
12. Oreanda-Isar, Mt Krestovaya	settlement	F	WC	500	AU, 0–5.5	4.86	135	0.270
					BCA, 5.5–14	4.86		
13. Kizil-Tash (Gelin-Kaya)	Fortress	F	WC	500	AU, 0–16	4.63	158	0.316
19. Fortress Sudak	Fortress	MHG	WC	500	–	–	230	0.460
17. Funa	Fortress	MHG	WC	500	AU, 0–18	3.44	145	0.290
21. Feodosia	Genoese fortress	MHG	WC	530	Av, 0–3.5	3.19	140	0.260
					A, 3.5–7.8	2.76		
					AC, 7.8–14	2.74		
7. Chembalo	Fortress	MHG	CaG	535	AU, 0–19	4.05	182	0.340
4. Chersonesos	near the Western Basilica	MHG	L	1000	AU, 0–15	6.34	150	0.150
11. Ai-Todor	monastery	MHG	WC	1000	AU, 0–6	1.27	155	0.155
					AC, 6–15.5	0.81		
15. Cape Plaka	remains of a church	F	WC	1000	AU, 0–13	2.66	270	0.270
14. Artek	settlement	F	WC	1400	–	–	150	0.107
16. Aluston	Fortress	MHG	WC	1400	–	–	158	0.113
9. Charax	upper wall	F	CaG	1650	AU, 0–16	4.92	224	0.136
					BCA, 16–31	4.86		
10. Charax	lower wall	MHG	WC	1650	AU, 0–7.5	5.04	160–190	0.100–0.115
					BCA, 7.5–16	4.81		
6. Farmhouse, Berman Ravine	settlement	MHG	L	1900	AU, 0–25	4.70	242	0.127
18. Kutlak	Fortress	MHG	L	2000	AU, 0–30	4.46	300	0.150
5. Chersonesean farmhouse (land plot 197)	settlement	MHG	WC	2280	AU, 0–30	1.90	288	0.126

[a]Numbers of archaeological sites correspond to the numbers in Figure 1.
[b]F – forest; MHG – mixed herbs and grasses.
[c]WC – weathering crust; CaG – clay and gravel; L – loam. Column 'Horizon' indicates the depth at which samples for C_{org}, % have been taken. Instances when C_{org}, % has not been measured are indicated with a dash.

Table 5. Chemical and geochemical parameters in the SCC soil chronosequences.

| Object (Figure 1)		2	1	1	1	7	6	6	5	5
Age, years		158	360	>		535	1900		2280	
Horizon, cm		0–11	0–14	14–35	37–	0–20	0–10	10–24	0–15	15–29
Dry soil Munsell colour		10YR 5/1	10YR 6/2	10YR 7/1		10YR 5/3	10YR 7/2	10YR 7/1	10YR 6/5	10YR 7/5
pH_{H2O}		7.5	7.9	8.1		7.9	7.9	8.2	8.1	8.2
$CaCO_3$	%	41.3	58.1	77.7		24.2	31.0	29.9	41.1	42.9
Sum of adsorbed bases, Including	mmol dm^{-3} per 100 g	22.10	18.08	13.35		20.40	21.96	21.29	26.36	22.92
Ca^{2+}	mmol dm^{-3} per 100 g	14.30	12.28	8.25		18.40	18.06	17.69	19.16	19.62
Mg^{2+}	mmol dm^{-3} per 100 g	7.80	5.80	5.10		0.60	3.90	3.60	7.20	3.30
Na^+	mmol dm^{-3} per 100 g	0.70	0.60	0.50		0.10	0.60	0.60	0.50	0.60
Humus	%	11.7	11.1	4.8		4.1	5.7	3.2	3.9	2.5
P_2O_5[a]	mg kg^{-1}	296.1	110.7	159.7		78.0	383.6	381.1	17.0	6.8
K_2O[a]	mg kg^{-1}	1810.8	248.1	107.2		1604.5	1454.5	1332.3	878.6	543.5
V	Ppm	46.88	35.18	28.46	30.20	91.10	50.71	48.53	58.46	64.23
Cr	Ppm	97.80	76.60	72.61	71.87	68.75	73.62	71.35	75.94	80.07
MnO	Ppm	1104.19	579.88	406.80	408.53	735.90	734.82	749.00	1039.12	923.26
Sr	Ppm	480.83	298.04	324.03	323.99	131.27	145.82	147.42	162.02	179.49
Zn	Ppm	222.63	90.68	73.65	71.67	124.85	110.76	112.78	98.92	96.48
Pb	Ppm	110.24	16.43	1.69	1.63	40.98	18.16	17.42	25.51	20.89
Ni	Ppm	55.94	21.42	12.58	14.08	59.68	38.94	39.16	49.38	51.65
As	Ppm	15.51	5.02	3.82	3.35	7.06	5.41	5.85	7.41	7.34
Cu	Ppm	33.46	3.34	bl	bl	49.81	24.40	27.56	43.30	40.21
Co	Ppm	7.88	Bl	bl	bl	bl	7.99	5.68	5.35	7.27
CaO	%	27.01	42.76	50.85	50.23	10.52	21.49	23.78	23.44	23.31
SiO_2	%	10.54	4.94	5.25	6.35	46.01	34.18	28.75	21.43	23.77
TiO_2	%	0.39	0.26	0.24	0.24	0.57	0.44	0.42	0.45	0.48
Al_2O_3	%	5.94	4.74	4.20	4.86	9.93	9.66	8.54	9.95	10.69
Fe_{total}	%	2.40	1.06	0.79	0.85	4.36	2.24	2.16	2.66	3.01
MgO	%	2.96	3.80	4.55	4.30	2.62	2.38	2.51	2.50	2.67
Na_2O	%	3.14	3.45	4.08	3.99	2.42	1.97	2.02	2.30	2.30
P_2O_5	%	1.53	0.77	0.69	0.68	0.55	0.89	0.89	0.26	0.22
K_2O	%	1.43	0.75	0.67	0.69	1.98	1.69	1.57	1.71	1.83
Geochemical indicators										
$Si/(Al + Fe + Mn)$		0.91	0.66	0.83	0.88	2.33	2.22	2.06	1.29	1.32
C_e		0.30	0.10	0.09	0.11	2.61	1.24	0.96	0.71	0.79

bl: below the determination level
[a]By Machigin method.

Table 6. Changes in the energy expenditures for soil formation ($\bar{Q}$) and potential variations in the humus-horizon thickness (ΔH_{lim}), by 90-year periods.

Period, years ago	$\bar{Q} \pm \theta$, MJ m^{-2} yr^{-1} (Rasmussen and Tabor, 2007)	$\bar{Q} \pm \theta$, MJ m^{-2} yr^{-1} (Volobuev, 1975)	ΔH_{lim}, mm	Period, years ago	$\bar{Q} \pm \theta$ (Rasmussen and Tabor, 2007)	$\bar{Q} \pm \theta$ (Volobuev, 1975)	ΔH_{lim}, mm
2500–2410	130.8 ± 52.1	920.9 ± 1.9	+30	1240–1150	145.8 ± 52.3	1029.8 ± 4.1	+73
2410–2320	129.2 ± 52.3	908.5 ± 1.1	−2	1150–1060	145.5 ± 52.2	1027.8 ± 3.1	−70
2320–2230	127.2 ± 52.3	893.2 ± 4.7	−40	1060–970	153.0 ± 52.3	1078.2 ± 5.3	+24
2230–2140	129.2 ± 52.3	909.1 ± 4.1	+63	970–880	157.8 ± 52.2	1108.9 ± 1.8	+37
2140–2050	125.8 ± 52.2	881.9 ± 3.6	−30	880–790	157.6 ± 52.3	1107.5 ± 3.6	−80
2050–1960	124.8 ± 52.3	874.4 ± 3.0	−42	790–700	166.3 ± 52.2	1161.5 ± 1.7	+72
1960–1870	128.5 ± 52.3	903.8 ± 4.3	+99	700–610	164.9 ± 52.1	1152.8 ± 1.0	−32
1870–1780	123.0 ± 52.1	859.7 ± 3.8	−106	610–520	167.4 ± 52.1	1167.9 ± 0.8	−1
1780–1690	128.8 ± 52.2	905.4 ± 1.0	+73	520–430	167.6 ± 52.1	1169.2 ± 0.7	−1
1690–1600	126.8 ± 52.2	890.5 ± 1.0	−41	430–340	167.7 ± 52.2	1169.7 ± 2.3	+30
1600–1510	130.6 ± 52.1	919.3 ± 3.4	+21	340–250	162.2 ± 52.1	1136.1 ± 1.6	−61
1510–1420	131.8 ± 52.2	929.0 ± 2.3	−23	250–160	163.8 ± 52.2	1146.0 ± 1.8	+75
1420–1330	136.7 ± 52.3	965.1 ± 0.6	+33	160–70	154.2 ± 52.3	1085.8 ± 4.4	−75
1330–1240	137.6 ± 52.2	971.8 ± 2.0	−57	70–0	153.5 ± 52.3	1081.3 ± 4.8	+31

θ: confidence interval for the average.
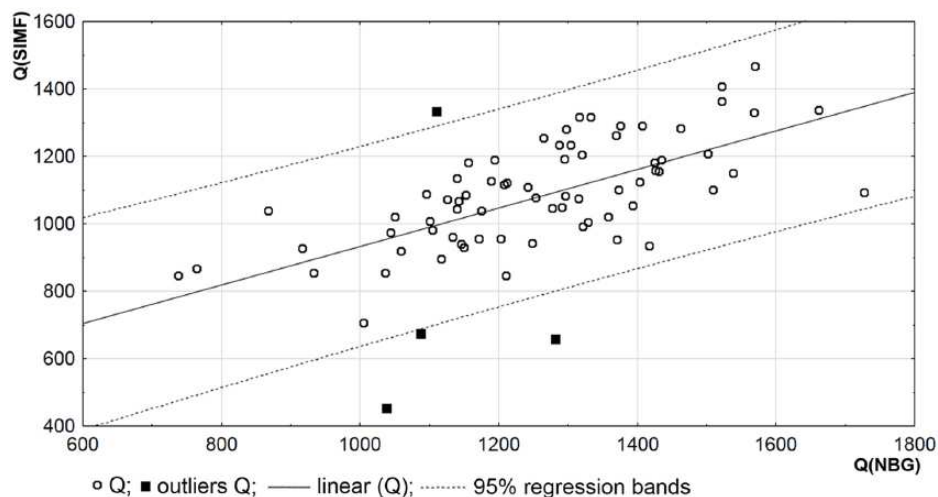
Figure 4. Correlation of energy expenditures for pedogenesis observed at weather stations in Simferopol (Q[SIMF]) and at the Nikitsky Botanical Garden (Q[NBG], MJ m^{-2} a^{-1}).

periodicity of climate change multiple to the solar activity cycles. In the dynamic series of the climate-controlled energy for pedogenesis, two qualitatively distinct periods can be defined (Figure 4). While the average value of Q for the period of 1887–2003 is 1116 MJ m^{-2} a^{-1}, in the period of 1887–1929, it amounts to 884 (687–1104) MJ m^{-2} a^{-1}, being considerably larger in the subsequent 74 years – 1251 (737–1727) MJ m^{-2} a^{-1} with a clear shift in variability. It seems that before and after 1930, we are dealing with two 80- to 90-year secular cycles which are known to be determined by the heliophysical and geomagnetic periodicity (Burlatskaya, 2002). Through decomposition of the time series using *Census I* method (Figure 5), a periodicity of 23 years is observed in the variation of the Q values.

Cycles with periods of 11 (Schwabe sunspot cycle), 22 (solar-magnetic or Hale cycle), 40 (30–35) (Brückner cycle) and 80–90 years (secular sunspot or Gleissberg cycle) have been determined in various high-resolution climatic archives (Beer et al., 1994; Damon and Sonett, 1991; Glenn and Kelts, 1991; Vos et al., 1997). The sunspot activity (SSN) is in general positively correlated with changes of the 11-year average temperatures, although there is a slight lag (Beer et al., 1994; Friis-Christensen and Svensmark, 1997; Lean et al., 1995).

In order to present the input data on a single scale, the time series of climate-controlled energy expenditures for pedogenesis (Q_c) and SSN were standardised. To evaluate the correlation and to reconstruct the energy expenditure for pedogenesis, the method of artificial neural network based on the architecture of generalised regression grid was applied. As a result, the GRNN architecture (1-81-2-1) has been obtained with a high reliability of the data restoration ($R = 0.87$). The basic periods and common regularities of the multi-annual solar activity, precipitation and pedogenesis were established by smoothing sequences with a 4253H filter. This filter includes several consecutive transformations: (1) four-point sliding median aligned by sliding median 2, (2) five-point sliding median, (3) three-point sliding median, (4) three-point weighed sliding average with weights (0.25, 0.5, 0.25), (5) calculation of the residues through the subtraction of the transformed series from the initial series, (6) steps 1–4 are repeated on the residues and (7) the transformed residues are added to the transformed series ensuring a high degree of the initial-series parameter preservation (trend and cyclic components). The cyclic constituents of the time series of climatic factors were determined through one-dimensional Fourier (DFT) analysis.

Decomposition of the time series using *Census I* method shows, for SSNs as well as for the Q values, a basic periodicity of
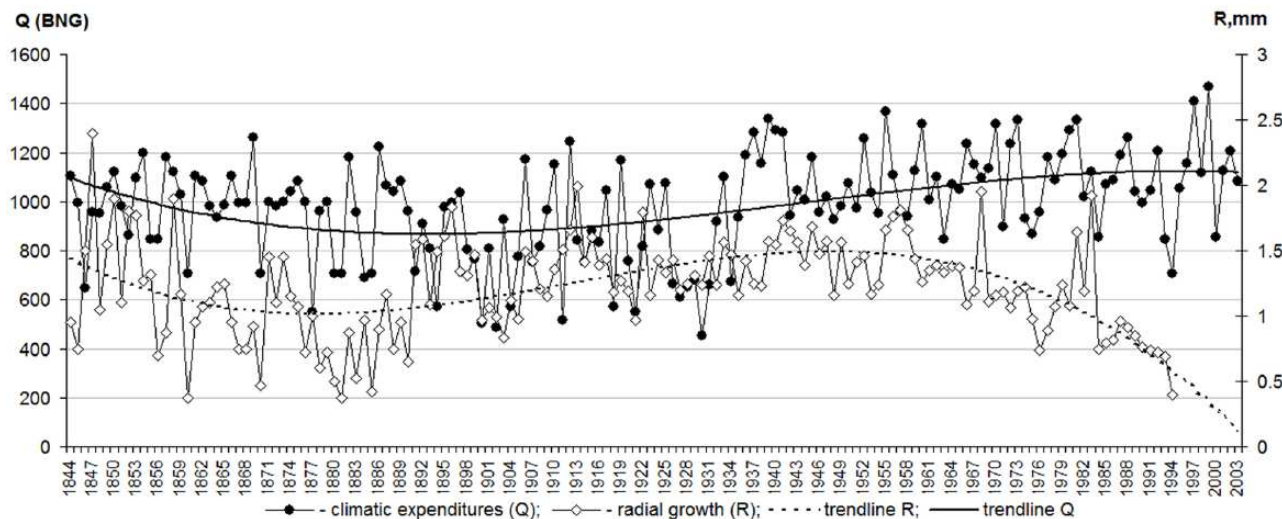
Figure 5. Year-to-year dynamics of long-term changes of energy expenditure for pedogenesis (Q[NBG], MJ m⁻² a⁻¹) and the juniper growth rates (*R*, mm).
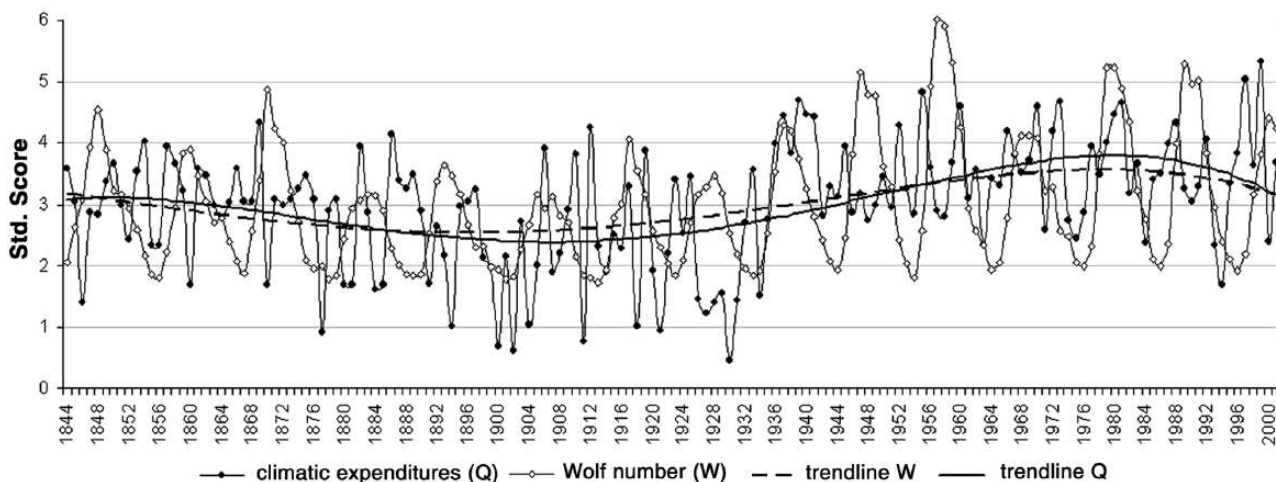

Figure 6. Year-to-year dynamics of long-term changes of energy expenditure for pedogenesis and solar activity (SSN). Note to axis Y: in standardisation, all values are replaced by standardised values, which are computed as follows: Standard Score = (raw score − mean)/standard deviation.

23 years. To define the nonlinear trend in the dependence of Q_c dynamics on SSN, a summarised (probabilistic) regression neural network was built. Given the complexity of the HF dynamics of Q_c, the maximum nonlinear correlation dependence of the dynamic series amounted to 0.52 (Figure 6). The linear correlation (R^2) of trend components of the two dynamic series is, however, 0.94, which suggests a direct response of Q_c to the SSN on the scale of intra-secular changes.

The transformation of the series allows us to identify two distinct periods in the dynamics of Q_c, which seem to be directly dependent on SSN: (1) AD 1844–1932 and (2) AD 1933–2001. In the second period, an average rise in SSN of 32.5% is observed, which, in turn, resulted in a 25.7% increase in climate-controlled energy expenditures for pedogenesis.

The examination of SSN based on the content of ¹⁴C in the annual growth rings of relict pines has shown (Ivanov and Lisetskiy, 1996) that the periods of minimum SSN and its persistent decrease (from maxima to minima) correspond to chronological spans with favourable ecological conditions for those regions where precipitation is a limiting factor.

In establishing the climate-pedogenesis relationship, the pedochronological data on the variations in the humus-horizon thickness (*H*, mm) and the organic carbon content (C_{org}, %) have been

used. The two chronosequences established are based on 23 objects with *H* ranging in age from 30 to 2000 years and 16 samples of C_{org} in the age range 105–2280 years.

Over the last 2.0 ka, the formation of the humus-horizon thickness was clearly undulant in its character (Figure 7a; model 3); less favourable conditions of pedogenesis 1.4–1.5 ka ago are replaced by higher rates of pedogenesis 0.5–0.7 ka ago.

The accumulation of C_{org} in the soil over time *t* is expressed as:

$$C_{org} = 7.931 \sin(0.0006006t + 1.776) + 2.994 \sin(0.002531t + 2.93), \quad r = 0.79$$

The one-dimensional Fourier (DFT) analysis demonstrates that the variations in the climate-controlled energy expenditures (*Q*) and in the humus-horizon thickness (*H*) have a similar duration of cycles: 1235, 823 and 617 years. This determines a relatively high relationship of their LF harmonic oscillations in the periods T_1, 280–930 years ago ($H_{t_1} = 0.982Q_t - 874.79$, $r = 0.84$), and T_2, 930–1720 years ago ($H_{t_2} = 0.157Q_t + 22.05$, $r = 0.62$). The average values of parameters for periods T_1 and T_2 amounted to $\overline{Q} = 1080$ MJ m⁻² yr⁻¹/$\overline{H} = 184$ mm and $\overline{Q} = 980$ MJ m⁻² yr⁻¹/$\overline{H} = 175$ mm, respectively. As a result of the cross-correlation
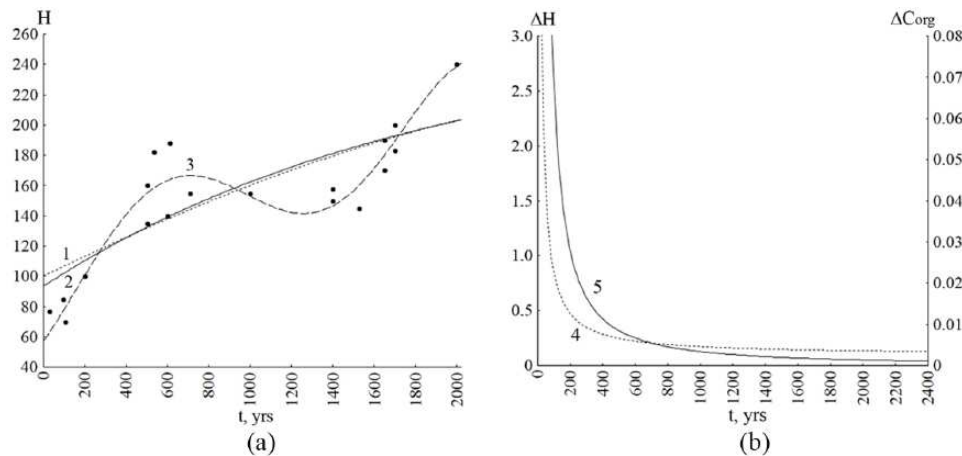
Figure 7. Changes in the humus-horizon thickness (*H*, mm) and the organic carbon content in the soil over time (*t*, years): (a) changes in H_t and (b) estimated speed of the humus-horizon formation and of the organic carbon accumulation in the soil (ΔC_{org}, % yr^{-1}): 1 – line function: $H_t = 260 \cdot \exp(-\exp(-0.050 - 0.00068t))$; $r = 0.78$; 2 – line function: $H_t = 260 \cdot (1 - 0.640 \cdot \exp(-0.00053t))$, $r = 0.79$; 3 – line function: $H_t = 646.6 \cdot \sin(0.001288t + 0.9629) + 595.8 \cdot \sin(0.001606t + 4.04) + 99.61 \cdot \sin(0.003168t + 6.21)$; 4 – line function: $f(\Delta H_t) = 70.2 \cdot t^{-0.986} + 0.096$, $r = 0.99$; 5 – line function: $f(\Delta C_{orgt}) = 26.32 \cdot t^{-1.293} - 6.214 \cdot 10^{-5}$, $r = 0.99$.

analysis, a 25- to 75-year inertial lag in the change of *H* has been revealed.

The accumulation of organic carbon in the humus horizon (Figures 5 and 7b) outpaces the formation of the humus horizon itself (Figures 4 and 7b) only in the first 700 years of pedogenesis. The intensive accumulation of C_{org} typical of the 'rapid growth' phase is replaced by an extensive growth of the humus profile, as an effect of stabilisation of the organic and mineral complex, that is, of its reaching the 'quasi-climax' state. This pattern is associated with the increasing role of eluvial and illuvial redistribution of humic substances along the profile and, thus, with a certain reduction in the concentration of C_{org} in the upper, accumulative horizon. Apart from the obvious, climate-conditioned differences in the speed of pedogenesis at different stages of soil formation, the above regularities confirm the soils' ability to change their functioning modes in response to external and internal factors. To reconstruct the LF changes in the soil profile, the connection between *Q* and *H* over the 400-year time period (1.6–2.0 ka ago) has been established; this time period has the genetically most similar harmonics. Then, the functional connection ($H = 1.2011Q + 890.87$, $r = 0.99$) has been established and the reconstruction for the period down to 2.5 ka ago has been made. The results are shown in Figure 8.

The humus-horizon formation of calcaric Cambisols is largely determined by climatic circles spanning from 600 (800) to 1200 years. This cyclicity, which is astroclimatic in its nature (Eddy, 1977) and manifests itself in the periodicity of pedogenesis in the Eastern Europe's steppe zone (Ivanov and Lisetskiy, 1996), may be considered evolutionarily significant even in conditions of relatively stable climate, as on the SCC.

Climate changes and other natural processes over time

The pollen and soil record of the south-western Crimea records a dry event between 4.2 and 3.3 ka BP (SB-2) (Cordova and Lehman, 2005; Gerasimenko and Subetto, 2007; Kostin, 1965), which is also represented in the pollen diagrams of south-eastern Ukraine (Gerasimenko, 1997). A considerable amelioration of the regional climate, accompanied by a decrease in summer temperature and an increase in precipitation, took place in the middle of the Sub-Atlantic (SA), around 1.1–0.8 ka BP (Kremenetski, 1995). In Crimea, the age of climatic phases is based on the varve chronology of Lake Saki (Šostakovič, 1934), partially supported by radiocarbon dates (Subetto et al., 2007). In SA, a number of

micro-stages were distinguished, including a cool and moist period of 2.6–2.2 ka BP and a warm and dry one in 2.2–1.6 ka BP, with the period of 2.2–1.9 ka BP proving to be the driest phase of the SA (Gerasimenko and Subetto, 2007).

The sediment deposits of Lake Saki offer a unique opportunity for linking time sequences of changing natural records (soils, bottom sediments) and regional climate fluctuations in the late Holocene. Our re-examination of relative secular variations in precipitation, the results of which are presented in Figure 8, is based on the 11-year filtered Lake Saki sedimentation intensity indices computed by Kostin (1965), which we have normalised using the weighted average (WA) and standard deviation (SD) of the annual sedimentation rate computed by secular intervals (WA = 1.4 mm, SD = 0.53 mm) as coefficients of standardisation. Linear relationship ($Q = 209.74 \cdot Still + 695.95$, $r = 0.63$) established on the basis of time series *Q* (BNG) and Still (Šostakovič, 1934) overlapping in the period of 1844–1894 made it possible to use the Saki Lake sedimentation rate data for reconstructing the climatic conditions (*Q*, MJ m^{-2} yr^{-1}) over the last 2.5 ka.

Based on the data presented in Figure 9, three distinct periods can be identified: (1) 4.5–3.2 ka ago – a period of a significant decrease in precipitation with a high degree of variation; (2) 3.2–1.25 ka ago – some increase in precipitation towards the middle of the period with a clearly expressed periodicity; and (3) 1.25 ka ago until the present – a significant increase in precipitation, particularly in the span 1.0–0.7 ka ago. The reconstructed rainfall variations correlate well with the pollen data from the Pontic lowland (Kremenetski, 1995, 2003) and palaeoclimatic evidence from Central Asia (Oberhänsli et al., 2007), being more often opposed to that from northern and central Europe as well as central Anatolia (Jones et al., 2006; Lamb, 1977). The statistically significant correlation between the thickness of Lake Saki varves and the *Pinus hamata D.Sosn* ring-width data spanning 1620–2002 confirms the value of lacustrine sediment archives as proxy for past precipitation in the region. If so, the wettest period of the last 1.5 ka (ca. AD 1050–1250) will coincide with the 'Medieval Warming' in Crimea (Solomina et al., 2005).

The existence of links between solar activity and climate, also reflected in varved lacustrine sediments, has been demonstrated by many studies, although the underlying physical mechanisms remain insufficiently understood (Gray et al., 2010; Hady, 2013; Hiremath, 2009; Menking, 2015; Vos et al., 1997). The periodogram analysis of the LF oscillations of SSN reveals two cycles with durations of 1230 and 540 years. The same method was applied to analyse the time series of the humus-horizon
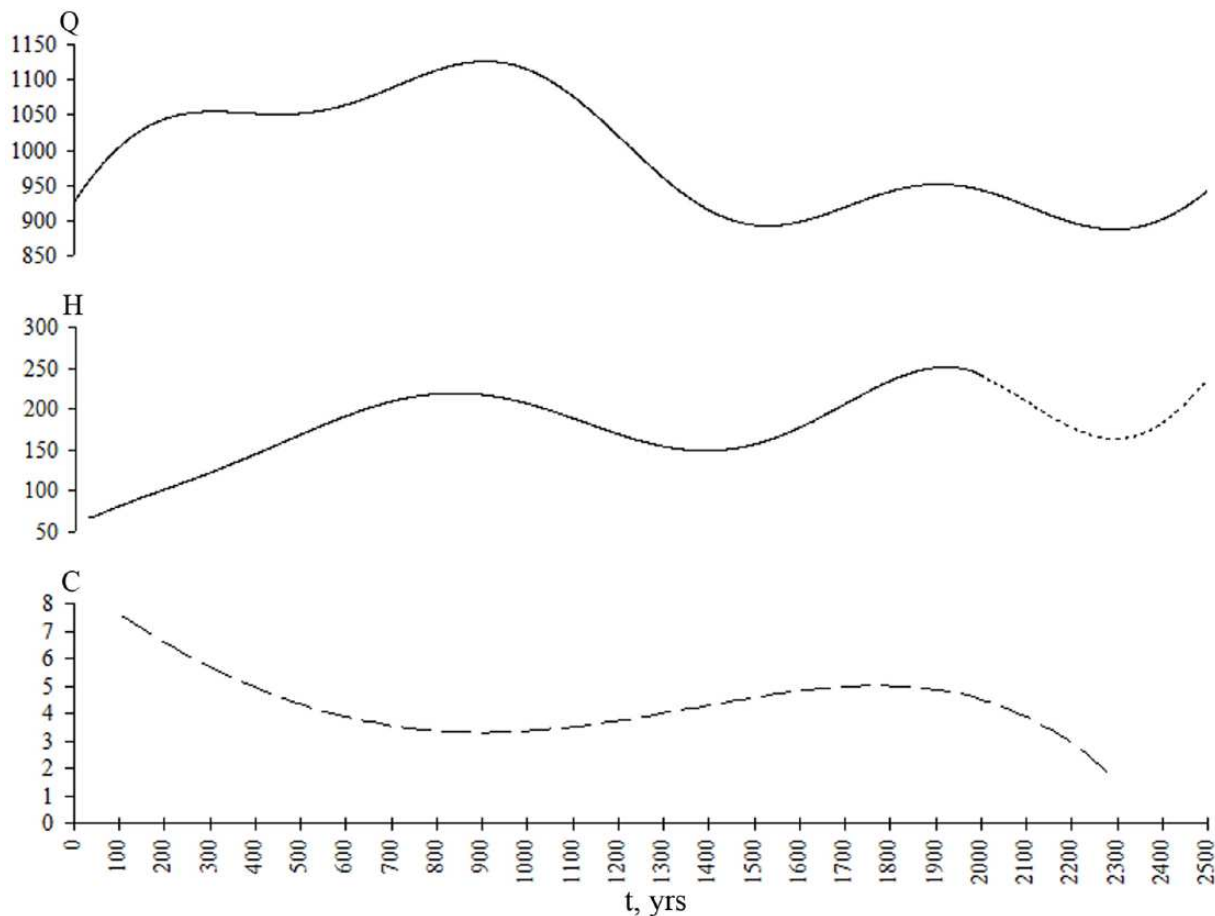
Figure 8. Reconstruction and synchronisation of low-frequency harmonics of the climate and soil-forming processes for the last 2500 years: Q – the energy intake on pedogenesis, MJ m^{-2} yr^{-1}; H – humus-horizon thickness, mm (the dotted line shows the forecast); and C_{org} – organic carbon content in the soil, %.

transformation in the steppe soils of southern Ukraine over 6000 years. This study has confirmed the previously established (Ivanov and Lisetskiy, 1996) negative correlation between these two processes, that is, the maxima of SSN correspond to the phases of intensive denudation when the sedimentation rate of lacustrine deposits increased. During the last 6.0 ka, three intervals favourable for pedogenesis are discernible in the millennial and submillennial scales, which, as suggested by the periodogram, are connected with cycles of 1350–1450 and 600/700–800 years.

Decomposition of the time series using symlet wavelet function of the eighth order was performed until the palaeotrends could be discerned, which made it possible to trace the harmonic oscillations at different levels of localisation, with DWT of approximating and refining signals using multiple-scale analysis. The resulting LF component of the variation in Q can be expressed as:

$$Q = 2090 \sin (0.000853t - 0.02484)$$
$$+ 1191 \sin (0.001311t + 2.243)$$
$$+ 52.52 \sin (0.006832t + 1.099), \quad r = 0.75$$

where r is coefficient of correlation between the initial data and the LF component values.

Throughout the SA, five micro-stages with an average duration of 400–600 years can be distinguished (Gerasimenko, 2007): 2.6–2.2, 2.2–1.6, 1.6–1.2, 1.2–0.8 and 0.8–0.15 ka BP. A spectrum analysis of over 4 ka-long Lake Saki varve record in 200-year swaths carried out by Currie (1995) provided evidence of two peaks with periods of 18.5 ± 1.5 years and 10.7 ± 0.8 years. These peaks were identified as the 18.6-year luni-solar and the 10- to 11-year solar cycle signals in climate, respectively. The

sunspot or Schwabe cycle of 11 years and periodic components of 14–16, 20–25, 44–46, 57–67, 120–130 and 200–250 have also been identified in this data in the analyses by others (Liritzis and Fairbridge, 2003; Xanthaki et al., 1995).

The existence of a relationship between climate and lake sedimentation rates in Crimea established by previous studies (Kostin, 1965; Lamb, 1977; Šostakovič, 1934) makes it possible to distinguish within the SA two phases of pedogenesis differing in terms of moisture provision: (1) 2.3–1.25 ka ago, when, because of the fact that arid and humid conditions fluctuated on a quasi-similar magnitude forming no steady climatic trend, pedogenesis was in a dynamic equilibrium; and (2) 1.25 ka ago to the present, when an increase in moisture (especially in 1.0–0.7 ka ago) determined an accelerated development of the SCC's soils.

Conclusion

The Fourier (DFT) analysis of intra-secular changes in climate-conditioned energy for pedogenesis demonstrated that the periodicity of this process is determined by two cyclic constituents of 23 and 80 years, which coincide with SSN periods of a similar duration, thus suggesting a possible explanation for the short-term climate changes. These periods express themselves at the functional level and determine the pedoclimate.

The identification of long-term evolutional changes requires more considerable duration of stable periods in natural processes. The study of sedimentation rates in Lake Saki over the period 3.2–1.25 ka ago suggests that the periodicity of sediment accumulation is related to five super-secular cycles, the duration of which seems to have been related (by doubling) to a 600-year cycle. A quasi-periodic component of about 500–700 years is found in the
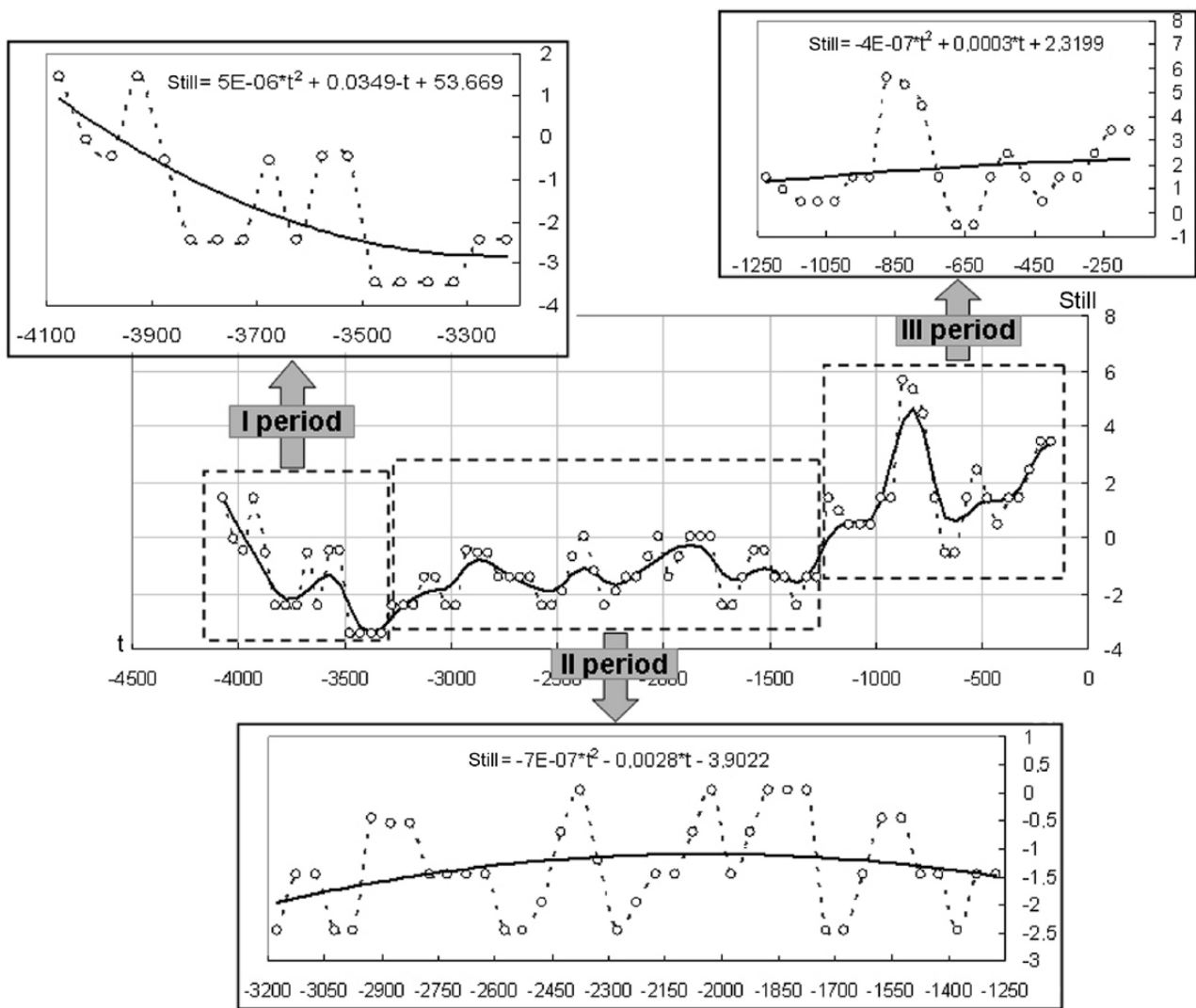
Figure 9. Relative secular variations in precipitation over the past 4000 years (*t*) based on the sedimentation rate data (Still, mm·10⁻¹) from Lake Saki (Kostin, 1965). Periods I–III – multi-centennial periods.

scheme of Eddy (1977), while the time gap between two neighbouring maxima of SSN in the most reliable historical period does not exceed 600 years. The existence of a 600-year cycle in SSN is confirmed by a similar repetition of high numbers of comets and by dendrochronological data (Veklič, 1987), as well as through the discovery of a period with an average duration of 554 years in simulation of 11-year sunspot cycles for the period since 648 BC (Vitinskij, 1973).

Wavelet decomposition of the climatic series made it possible to identify three levels of LF signals used for the retrospective reconstruction of climatic harmonics for the last 2.5 ka of the natural environment evolution in the SCC. Using one-dimensional Fourier analysis (DFT), the main periods of 830, 625, 250, 192 and 90 years have been identified and a 90-year Parzen-window filtration was performed.

In the general direction of the soil-formation process, three main stages can be identified: (1) 2500–1780 years ago – a slight decrease in energy expenditures for soil formation (Q) (by 61.2 MJ m⁻² yr⁻¹ on average); (2) 1780–340 years ago – an essential rise in Q (by 310.0 MJ m⁻² yr⁻¹ on average); and (3) 340 years ago to present – a decrease in Q (by 88.4 MJ m⁻² yr⁻¹ on average).

The human impact on the SCC landscape suggested by various proxies is not directly reflected in the newly formed soils, which have developed on top of archaeological sites, and were the primary focus of this study. The evaluation of this impact is also hampered by massive erosion and alluviation processes, which, as in other regions, might have entirely buried the traces of human activity (Carter, 2006), thus introducing a potential bias into the present notion of human occupation on the SCC. Beside its impact on pedogenesis, climate change, directly or indirectly, has contributed to the nonlinear development and the discontinuity in human settlement in the area. The driest phase of the SA (2.2–1.9 ka ago) coincides with a clear decrease of human activity on the SCC. To better comprehend the human impact on the Crimean coastal landscape, the analyses of newly formed soils need to be complemented by the studies of geomorphological developments and buried soils.

Acknowledgements

Funding

References

Alyabina IO and Nedanchuk IM (2014) Assessment of the relationships between the distribution of soil horizons and the climatic parameters. *Eurasian Soil Science* 10: 968–979.

Arinushkina EV (1970) *Manual for the Chemical Analysis of Soils*. Moscow: University Press (in Russian).

Bagrov NV and Rudenko LG (eds) (2004) *Atlas: The Autonomous Republic of Crimea*. Kyiv; Simferopol: Taurida National V.I. Vernadsky University.

Bagrova LA, Bokov VA and Bagrov NV (2001) *Geografija Kryma*. Kiev: Lybid.

Bagrova LA, Bokov VA, Garkuša LJ et al. (2003) Krymskoe Subsredizemnomor'e. In: Mišnev VG and Oliferov AN (eds) *Ekosistemy Kryma, ich optimizacija i ochrana*. Simferopol: Tavričeskij Nacional'nyj universitet, pp. 95–105.

Beer J, Joos F, Lukasczyk C et al. (1994) [10]Be as an indicator of solar variability and climate. In: Nesme-Ribes E (ed.) *The Solar Engine and Its Influence on Terrestrial Atmosphere and Climate*. Berlin, Heidelberg: Springer, pp. 221–233.

Berezina LS (ed.) (1967) *Spravočnik po klimatu SSSR. Volume 10, Parts 1–4*. Leningrad: Gidrometeoizdat.

Bibikova VI (1970) Fauna iz poselenija u s. Kirova. In: Leskov AM (ed.) *Drevnosti Vostočnogo Kryma (predskifskij period i skify)*. Kiev: Naukova dumka, pp. 97–112.

Bilde PG, Attema P and Winther-Jacobsen K (eds) (2012) *Dzharyl-gach Survey Project*. Aarhus: Aarhus University Press.

Blavatskij VD (1951) *Charaks* (Materialy i issledovanija po archeologii SSSR 19). Moscow: Nauka.

Brooks CEP (1949) *Climate through the Ages*. London: Benn Ltd.

Burlatskaya SP (2002) The geomagnetic field variation pattern over the last 6500 years. *Izvestiya, Physics of the Solid Earth* 5: 363–370.

Butzer KW (2005) Environmental history in the Mediterranean world: Cross-disciplinary investigation of cause-and-effect for degradation and soil erosion. *Journal of Archaeological Science* 32: 1773–1800.

Carter JC (ed.) (2002) *The Study of Ancient Territories: Chersonesos and Metaponto – 2002 Annual Report*. Austin, TX: Institute of Classical Archaeology, the University of Texas.

Carter JC (2006) Towards a comparative study of chorai west and east: Metapontion and Chersonesos. In: Guldager Bilde P and Stolba VF (eds) *Surveying the Greek Chora: The Black Sea Region in a Comparative Perspective*. Aarhus: Aarhus University Press, pp. 175–205.

Carter JC, Crawford M, Lehman P et al. (2000) The chora of Chersonesos in Crimea, Ukraine. *American Journal of Archaeology* 104: 707–741.

Cordova CE and Lehman PH (2003) Archaeopalynology of synanthropic vegetation in the chora of Chersonesos, Crimea, Ukraine. *Journal of Archaeological Science* 30: 1483–1501.

Cordova CE and Lehman PH (2005) Holocene environmental change in southwestern Crimea (Ukraine) in pollen and soil records. *The Holocene* 15: 263–277.

Cordova CE and Lehman PH (2006) Mediterranean agriculture in south-western Crimea: Palaeo-environments and early adaptations. In: Peterson DL, Popova LM and Smith AT (eds) *Beyond the Steppe and the Sown. Proceedings of the 2002 University of Chicago Conference on Eurasian Archaeology*. Leiden; Boston, MA: Brill, pp. 425–447.

Currie RG (1995) Luni-solar and solar cycle signals in lake Saki varves and further experiments. *International Journal of Climatology* 15: 893–917.

Damon PE and Sonett CP (1991) Solar and terrestrial components of the atmospheric ^{14}C variation spectrum. In: Sonett CP and Giampapa MS (eds) *The Sun in Time*. Tucson, AZ: University of Arizona Press, pp. 360–388.

Eddy JA (1977) Climate and the changing sun. *Climatic Change* 1: 173–190.

Ena VG, Ena AIV and Ena AnV (2007) *Otkryvateli zemli Krymskoj*. Simferopol: Biznes–Inform.

Fedorov VN (2010) Struktura mnogoletnich kolebanij stoka r. Dnepr po materialam donnych otloženij Sakskogo ozera. In: Koronkevič NI, Barabanova EA and Zajceva IS (eds) *Ekstremal'nye gidrologičeskie situacii*. Moscow: Media-Press, pp. 125–136.

Friis-Christensen E and Svensmark H (1997) What do we really know about the Sun-climate connection? *Advances in Space Research* 20: 913–921.

Fritts D (1976) *Tree Rings and Climate*. New York: Academic Press.

Gerasimenko NP (1997) Environmental and climatic changes between 3 and 5 ka BP in Southeastern Ukraine. In: Dalfes HN, Kukla G and Weiss H (eds) *Third Millennium BC Climate Change and Old World Collapse* (NATO ASI series 49). Berlin, Heidelberg: Springer, pp. 371–399.

Gerasimenko NP (2007) Landšaftno-klimatyčni zminy na teritorii Ukrainy za ostanni 2.5 tys. rokiv. In: *Istoryčna geografija: počatok XXI stolittja*. Vinnitsa: Teza, pp. 41–53.

Gerasimenko NP and Subetto DA (2007) Vegetational and climatic changes in the south-western Crimea during the Middle-Late-Holocene, based on pollen study of Lake Saki. In: Yanko-Hombach V (ed.) *Extended Abstracts IGCP 521–481 Joint Meeting and Field Trip*, Gelendzhik-Kerch, September 8–17, 2007. Moscow: Rosselkhozakademiya Printing House, pp. 69–71.

Glenn CR and Kelts K (1991) Sedimentary rhythms in lake deposits. In: Einsele G, Ricken W and Seilacher A (eds) *Cycles and Events in Stratigraphy*. Berlin, Heidelberg: Springer, pp. 188–221.

Goleusov PV and Lisetskii FN (2009) *Soil Reproduction in the Anthropogenically Disturbed Forest-Steppe Landscapes*. Moscow: GEOS.

Gray LJ, Beer J, Geller M et al. (2010) Solar influences on climate. *Reviews of Geophysics* 48: RG4001.

Hady AA (2013) Deep solar minimum and global climate changes. *Journal of Advanced Research* 4: 209–214.

Haykin S (2008) *Neural Networks: A Comprehensive Foundation*. 2nd Edition. New Delhi: Prentice Hall of India.

Hiremath KM (2009) Solar forcing on the changing climate. *Sun and Geosphere* 4: 16–21.

IUSS Working Group WRB (2014) *World Reference Base for Soil Resources 2014. International Soil Classification System for Naming Soils and Creating Legends for Soil Maps*. World Soil Resources Reports no. 106. Rome: FAO.

Ivanov IV and Lisetskiy FN (1996) Correlation of soil formation rhythms with periodicity of solar activity over the last 5000 years. *Transactions (Doklady) of the Russian Academy of Sciences: Earth Science Sections* 340(1): 189–194.

Januševič ZV (1986) *Kul'turnye rastenija Severnogo Pričernomor'ja. Paleoetnobotaničeskie issledovanija*. Kišinev: Štiinca.

Jenny H (1980) *The Soil Resource: Origin and Behavior*. New York: Springer.

Jones MD, Roberts CN, Leng MJ et al. (2006) A high-resolution late-Holocene lake isotope record from Turkey and links to North Atlantic and monsoon climate. *Geology* 34: 361–364.

Kočkin MA (1967) *Počvy, lesa i klimat Gornogo Kryma i puti ich racional'nogo ispol'zovanija* (Naučnye trudy Nikitskogo Botaničeskogo Sada, 38). Moscow: Kolos.

Kočkin MA and Novikova AV (eds) (1969) *Soils of the Crimean Oblast*. Simferopol: Krym.

Kočkin MA, Važov VI and Ivanov VF (1972) *Osnovy racional'nogo ispol'zovanija počvenno-klimatičeskich uslovij v zempledelii*. Moscow: Kolos.

Kolotuchin VA (1996) *Gornyj Krym v epochu pozdnej bronzy – načale železnogo veka*. Kiev: Južnogorodskie Vedomosti.

Kolotuchin VA (2003) *Pozdnij bronzovnyj vek Kryma*. Kiev: Stilos.

Korsakova S (2011) Impact of climate change on the grape productivity in the Southern coast of the Crimea. In: Attri SD, Rathore LS, Sivakumar MVK et al. (eds) *Challenges and Opportunities in Agrometeorology*. Berlin, Heidelberg: Springer, pp. 385–396.

Kostin SI (1965) Kolebanija klimata na Russkoj ravnine v istoričeskuju epochu. *Trudy Glavnoj Geofizičeskoj Observatorii* 181: 56–74.

Kravčenko E (2008) *Kyzyl-kobyns'ka kultura u Zachidnomu Krymu* (Abstract). PhD Thesis. Kyiv: Instytut archeologii NAN Ukrainy.

Kremenetski CV (1995) Holocene vegetation and climate history of southwestern Ukraine. *Review of Palaeobotany and Palynology* 85: 289–301.

Kremenetski CV (2003) Steppe and forest-steppe belt of Eurasia: Holocene environmental history. In: Levine M, Renfrew C and Boyle K (eds) *Prehistoric Steppe Adaptation and the Horse*. Cambridge: McDonald Institute for Archaeological Research, pp. 11–27.

Kris CI (1981) *Kizil-Kobinskaja kul'tura i tavry* (SAI D1–7). Moscow: Nauka.

Lamb HH (1977) *Climate: Present, Past and Future, Volume 2: Climatic History and the Future*. London: Methuen.

Lean J, Beer J and Bradley RS (1995) Reconstruction of solar irradiance since 1610: Implications for climate change. *Geophysical Research Letters* 22: 3195–3198.

Liritzis I and Fairbridge R (2003) Remarks on astrochronology and time series analysis of Lake Sake varved sediments. *Journal of the Balkan Geophysical Society* 6: 165–172.

Lisetskii FN and Ergina EI (2010) Soil development on the Crimean Peninsula in the Late-Holocene. *Eurasian Soil Science* 6: 601–613.

Lisetskii FN, Stolba VF and Goleusov PV (2016) Modeling of the evolution of steppe chernozems and development of the method of pedogenetic chronology. *Eurasian Soil Science* 49: 846–858.

Lisetskii F, Stolba VF and Marinina O (2015) Indicators of agricultural soil genesis under varying conditions of land use, Steppe Crimea. *Geoderma* 239–240: 304–316.

Lisetskii FN, Stolba VF and Pichura VI (2013a) Periodicity of climatic, hydrological and lacustrine sedimentation processes in the south of the East-European Plain. *Regional Environmental Issues* 4: 19–25.

Lisetskii FN, Stolba VF, Ergina EI et al. (2013b) Post-agrogenic evolution of soils in ancient Greek land use areas in the Herakleian Peninsula, south-western Crimea. *The Holocene* 23: 504–514.

Liu G, Li L, Wu L et al. (2009) Determination of soil loss tolerance of an entisol in Southwest China. *Soil Science Society of America Journal* 73: 412–417.

Lovelius NV and Grican JI (1998) *Lesnye ekosistemy Ukrainy i teplo-vlagoobespečennost'*. St Petersburg: PANI.

Luterbacher J, Dietrich D, Xoplaki E et al. (2004) European seasonal and annual temperature variability, trends, and extremes since 1500. *Science* 303(5663): 1499–1503.

Lysenko AV (2010) 'Poselenija' rimskogo vremeni Aluštinskoj doliny. In: Zajcev JP and Puzdrovskij AE (eds) *Drevnjaja i srednevekovaja Tavrika*. Donetsk: Donbass, pp. 259–277.

Maheras P (1988) Changes in precipitation conditions in the western Mediterranean over the last century. *Journal of Climatology* 8: 179–189.

Maheras P (1989) Principal component analysis of western Mediterranean air temperature variations 1866–1985. *Theoretical and Applied Climatology* 39: 137–145.

Menking KM (2015) Decadal to millennial-scale solar forcing of Last Glacial Maximum climate in the Estancia Basin of central New Mexico. *Quaternary Research* 83: 545–554.

Michaelsen J, Haston L and Davis FW (1987) 400 years of central California precipitation variability reconstructed from tree rings. *Water Resources Bulletin* 23: 809–818.

Motuzaite-Matuzeviciute G, Telizhenko S and Jones MK (2013) The earliest evidence of domesticated wheat in the Crimea at Chalcolithic Ardych–Burun. *Journal of Field Archaeology* 38: 120–128.

Myc VL (1989) Pozdneantičnye pamjatniki Aluštinskoj doliny. In: Vachtina MJ, Vinogradov JA and Zuev VJ (eds) *Skifija i Bospor*. Novočerkassk, pp. 77–79.

Myc VL (1991) *Ukreplenija Tavriki X–XV vv*. Kiev: Naukova dumka.

Nikolaenko GM (2006) The chora of Tauric Chersonesos and the cadastre of the 4th–2nd century BC. In: Bilde PG and Stolba VF (eds) *Surveying the Greek Chora: Black Sea Region in a Comparative Perspective*. Aarhus: University Press, pp. 151–174.

Novičenkov VI and Novičenkova NG (2002) O nižnej oboronitel'noj stene rimskoj kreposti Charaks. *Materialy po Archeologii, Istorii i Etnografii Tavrii* 9: 27–36.

Oberhänsli H, Boroffka N, Sorrel P et al. (2007) Climate variability during the past 2,000 years and past economic and irrigation activities in the Aral Sea basin. *Irrigation and Drainage Systems* 21: 167–183.

Rasmussen C (2012) Thermodynamic constraints on effective energy and mass transfer and catchment function. *Hydrology and Earth System Sciences* 3: 725–739.

Rasmussen C and Tabor NJ (2007) Applying a quantitative pedogenic energy model across a range of environmental gradients. *Soil Science Society of America Journal* 71(6): 1719–1729.

Rasmussen C, Southard RJ and Horwath WR (2005) Modeling energy inputs to predict pedogenic environments using regional environmental databases. *Soil Science Society of America Journal* 69(4): 1266–1274.

Ščeglov AN (1981) Tavry i grečeskie kolonii v Tavrike. In: Lordkipanidze OD (ed.) *Demografičeskaja situacija v Pričernomor'e v period Velikoi grečeskoi kolonizacii*. Tbilisi: Mecniereba, pp. 204–218.

Scholl T and Zinko V (1999) *Archaeological Map of Nymphaion (Crimea)*. Warsaw: Institute of Archaeology and Ethnology, Polish Academy of Sciences.

Schultz PN (1957) Tavrskoe ukreplennoe poselenie na gore Koška v Krymu. *Kratkie soobščenija Instituta Archeologii AN UkrSSR* 7: 62–66.

Solomina O, Davi N, D'Arrigo R et al. (2005) Tree-ring reconstruction of Crimean drought and lake chronology correction. *Geophysical Research Letters* 32(19): L19704.

Šostakovič BV (1934) Ilovye otloženija ozer i periodičeskie kolebanija v javlenijach prirody. *Zapiski Gosudarstvennogo Gidrologičeskogo Instituta* 13: 95–140.

Stolba VF (1993) Demografičeskaja situacija v Krymu v 5–2 vv. do n.e. (po dannym pis'mennych istočnikov). *Peterburgskij Archeologičeskij Vestnik* 6: 59–61.

Stolba VF (2002) Handmade pottery. In: Hannestad L, Stolba VF and Ščeglov AN (eds) *Panskoye I: Volume 1 – The Monumental Building U6*. Aarhus: Aarhus University Press, pp. 180–200.

Stolba VF (2005a) Monetary crises in the early Hellenistic poleis of Olbia, Chersonesos and Pantikapaion. A re-assessment. In: Alfaro C, Marcos C and Otero P (eds) *XIII Congreso Internacional de Numismática, Madrid 2003. Actas−Proceedings−Actes*. Madrid: Ministerio de Cultura, pp. 395–403.

Stolba VF (2005b) The oath of Chersonesos and the Chersonesean economy in the early Hellenistic period. In: Archibald

ZH, Davis JK and Gabrielsen V (eds) *Making, Moving and Managing: The New World of Ancient Economies, 323–31 BC*. Oxford: Oxbow, pp. 298–321.

Stolba VF (2012) La vie rural en Crimée antique: Panskoe et ses environs. *Études de Lettres* 1–2: 311–364.

Stolba VF (2014) *Greek Countryside in Ancient Crimea: Chersonesean Chora in the Late Classical to Early Hellenistic Period*. Aarhus: Faculty of Arts.

Stolba VF, Andresen J, Lisetskii FN et al. (2013) Surveys in the Chernomorskoye District, Crimea, Ukraine. In: Kozak DN (ed.) *Archaeological Researches in Ukraine, 2012*. Kyiv-Luc'k: Volyns'ky starožytnosti, pp. 87–89.

Stupko MV (2011) Nachodki kamennych sverlenych toporov-molotkov v Sevastopol'skom rajone. *Chersonesskij Sbornik* 16: 193–207.

Subetto DA, Stolba VF, Neustrueva IYu et al. (2007) Environmental and Black Sea level changes in the Holocene as recorded in Lakes Saki and Dzharylgach, Crimean Peninsula. In: Yanko-Hombach V (ed.) *Extended Abstracts IGCP 521–481 Joint Meeting and Field Trip, Gelendzhik-Kerch, September 8–17, 2007*. Moscow: Rosselkhozakademiya Printing House, pp. 157–159.

Subetto DA, Gerasimenko NP, Bakhmutov VG et al. (2009) Rekonstrukcija paleogeografičnych umov Zachidnogo Krymu u pizn'omu goloceni za litologičnymy i paleontologičnymy materialamy vyvčennja ozer. *Fizyčna geografija ta geomorfologija* 56: 299–310.

Švec GI (1974) *Mnogovekovaja izmenčivost' stoka Dnepra*. Leningrad: Gidrometeoizdat.

Telegin DY (1985) *Pamjatniki epochi mezolita na territorii Ukrainskoj SSR*. Kiev: Naukova dumka.

Veklič MF (1987) *Problemy paleoklimatologii*. Kiev: Naukova dumka.

Vernander NB (1986) Počvy Gornogo Kryma. In: Vernander NB and Tjutjunnik DA (eds) *Priroda Ukrainskoj SSR. Počvy*. Kiev: Naukova dumka, pp. 132–144.

Vitinskij JI (1973) *Cikličnost' i prognozy solnečnoj aktivnosti*. Leningrad: Nauka.

Volobuev VR (1975) *Introduction to Energetics of Soil Formation*. Cairo: Franklin Book Programs.

Vos H, Sanchez A, Zolitschka B et al. (1997) Solar activity variations recorded in varved sediments from the crater lake of Holzmaar – A maar lake in the Westeifel volcanic field, Germany. *Survey in Geophysics* 18: 163–182.

Xanthakis J, Liritzis I and Poulakos C (1995) Solar-climatic cycles in the 4,190-year Lake Saki mud layer thickness record. *Journal of Coastal Research* (Special issue) 17: 79–86.

Yanuchevitch Z, Nikolayenko G and Kuzminova N (1985) La viticulture à Chersonèse Taurique aux IVe–IIe siècles av. n.è. d'après les recherches archéologiques et paléoethnobotaniques. *Revue archéologique* 1: 115–122.

Zhang Z (2015) Tree-rings, a key ecological indicator of environment and climate change. *Ecological Indicators* 51: 107–116.

Zubar VM (2001–2002) Rimskoe voennoe prisutstvie v Tavrike. *Stratum plus* 4: 8–179.